The Astrophysical Journal Letters, 837:L21 (6pp), 2017 March 10 https://doi.org/10.3847/2041-8213/aa62aa

Dust in the Reionization Era: ALMA Observations of a $z = 8.38$ Gravitationally Lensed Galaxy

N. Laporte[1,2,3], R. S. Ellis[1,4], F. Boone[5,6], F. E. Bauer[2,3,7], D. Quénard[8], G. W. Roberts-Borsani[1], R. Pelló[5,6], I. Pérez-Fournon[9,10], and A. Streblyanska[9,10]

[1] Department of Physics and Astronomy, University College London, Gower Street, London WC1E 6BT, UK
[2] Instituto de Astrofísica and Centro de Astroingeniería, Facultad de Física, Pontificia Universidad Católica de Chile, Casilla 306, Santiago 22, Chile
[3] Millennium Institute of Astrophysics (MAS), Nuncio Monseñor Sótero Sanz 100, Providencia, Santiago, Chile
[4] European Southern Observatory (ESO), Karl-Schwarzschild-Strasse 2, D-85748 Garching, Germany
[5] Université de Toulouse, UPS-OMP, IRAP, Toulouse, France
[6] CNRS, IRAP, 14, avenue Edouard Belin, F-31400 Toulouse, France
[7] Space Science Institute, 4750 Walnut Street, Suite 205, Boulder, CO 80301, USA
[8] School of Physics and Astronomy Queen Mary, University of London, 327 Mile End Road, London E1 4NS, UK
[9] Instituto de Astrofísica de Canarias, C/Vía Láctea, s/n, E-38205 San Cristóbal de La Laguna, Tenerife, Spain
[10] Universidad de La Laguna, Dpto. Astrofísica, E-38206 La Laguna, Tenerife, Spain

Received 2017 January 21; revised 2017 February 21; accepted 2017 February 21; published 2017 March 8

Abstract

We report on the detailed analysis of a gravitationally lensed Y-band dropout, A2744_YD4, selected from deep *Hubble Space Telescope* imaging in the Frontier Field cluster Abell 2744. Band 7 observations with the Atacama Large Millimeter/submillimeter Array (ALMA) indicate the proximate detection of a significant 1 mm continuum flux suggesting the presence of dust for a star-forming galaxy with a photometric redshift of $z \simeq 8$. Deep X-SHOOTER spectra confirms the high-redshift identity of A2744_YD4 via the detection of Lyα emission at a redshift $z = 8.38$. The association with the ALMA detection is confirmed by the presence of [O III] 88 μm emission at the same redshift. Although both emission features are only significant at the 4σ level, we argue their joint detection and the positional coincidence with a high-redshift dropout in the *Hubble Space Telescope* images confirms the physical association. Analysis of the available photometric data and the modest gravitational magnification ($\mu \simeq 2$) indicates A2744_YD4 has a stellar mass of $\sim 2 \times 10^9\ M_\odot$, a star formation rate of $\sim 20\ M_\odot\ \mathrm{yr}^{-1}$ and a dust mass of $\sim 6 \times 10^6\ M_\odot$. We discuss the implications of the formation of such a dust mass only $\simeq$200 Myr after the onset of cosmic reionization.

Key words: early universe – galaxies: evolution – galaxies: formation – galaxies: high-redshift – galaxies: star formation – submillimeter: galaxies

1. Introduction

The first billion years of cosmic history represents the final frontier in assembling a coherent physical picture of early galaxy formation, and considerable progress has been enabled through observations from space-based telescopes and ground-based optical and near-infrared spectrographs. Early progress in the *Hubble* Ultra Deep and the CANDELS fields (Ellis et al. 2013; Bouwens et al. 2015; Finkelstein et al. 2015) has been complemented by surveys through lensing clusters (Postman et al. 2012), an approach culminating in *Hubble Space Telescope*'s (*HST*) flagship program, the Frontier Fields (FF; Lotz et al. 2016). By harnessing the magnification of a foreground massive cluster, galaxies of more representative luminosities can be probed (e.g., Laporte et al. 2014, 2016; Atek et al. 2015; Coe et al. 2015). Collectively, the blank field and cluster surveys have located several hundred star-forming galaxies in the redshift range $6 < z < 10$ corresponding to the era when it is thought hydrogen was photoionized (Robertson et al. 2015; Planck Collaboration et al. 2016). In addition to the population demographics analyzed through photometric data from *HST* and the *Spitzer Space Telescope*, spectroscopic diagnostics are being gathered to gauge the nature of their stellar populations and their capability for releasing the necessary number of ionizing photons (for a recent review, see Stark 2016).

The completion of the Atacama Large Millimeter/submillimeter Array (ALMA) brings the possibility of measuring the dust content of these early systems. Dust is likely produced by the first supernovae, and timing its formation would measure the extent of previous star formation. Moreover, dust can affect many of the key physical properties derived from photometric data. While early ALMA observations focused on distant $z \simeq 6$ massive ultra-luminous galaxies, targeting the more representative lower-mass systems in the reionization era brought into view by gravitational lensing is an interesting approach. An exciting early result was the detection of a significant dust mass in a $z \simeq 7.5$ galaxy whose rest-frame UV colors indicated little or no reddening (Watson et al. 2015).

The present Letter is concerned with the follow-up and analysis of an ALMA continuum detection in the FF cluster Abell 2744 close to a Y-band dropout, A2744_YD4, at a photometric redshift of $z \simeq 8.4$. In Section 2, we introduce the ALMA 1 mm continuum detection and its possible association with A2744_YD4 and justify a photometric redshift of $z \simeq 8$ for this galaxy. In Section 3, we analyze deep X-Shooter spectra that confirm the redshift via the detection of Lyα emission supported by O [III] 88 μm emission within the Band 7 ALMA data. We deduce the physical properties and dust mass of A2744_YD4 in Section 4 and discuss the implications for early dust formation in 5. Throughout this Letter, we use a concordance cosmology ($\Omega_M = 0.3, \Omega_\Lambda = 0.7$,

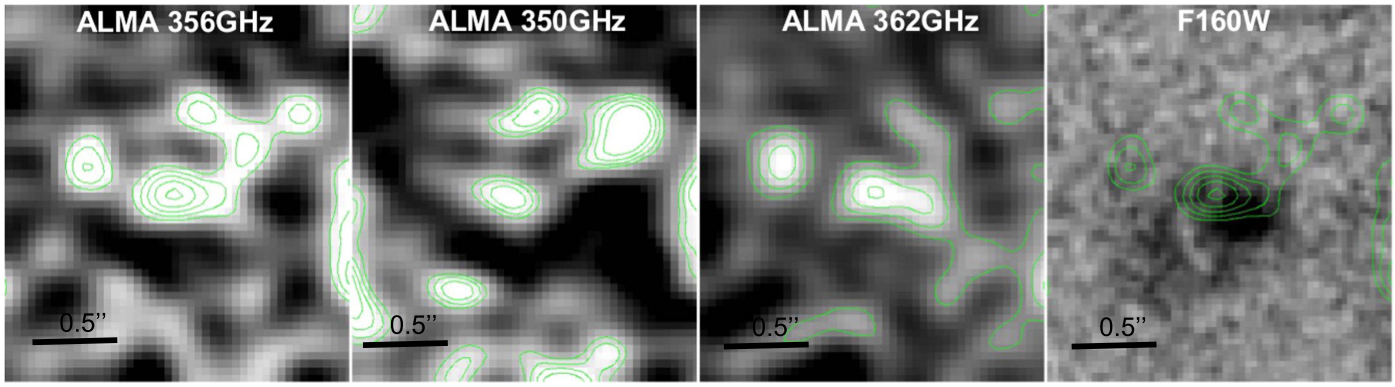

Figure 1. ALMA Band 7 continuum detection for A2744_YD4. (left) Map combining all frequency channels; (middle left and middle right) independent maps for two equal frequency ranges. Contours are shown at 1, 2, 3, 4, and 5σ adopting a noise level from an area of 0.5 × 0.5 arcmin. (right) *HST* F160W image with combined ALMA image contours overplotted.

and $H_0 = 70\ \mathrm{km\ s^{-1}\ Mpc^{-1}}$), and all magnitudes are quoted in the AB system (Oke & Gunn 1983).

2. Imaging Data

Here, we describe the ALMA data in which a high-z candidate is detected at 0.84 mm and the public imaging data used to constrain its spectral energy distribution (SED).

2.1. Deep ALMA Band 7 Observations

A deep ALMA Band 7 map (ID 2015.1.00594, PI: Laporte) of the FF cluster Abell 2744 centered at 0.84 mm ($f_c = 356$ GHz) was observed on 2016 July during 2.5 hr. The data were reduced using the CASA pipeline (McMullin et al. 2007) with a natural weighting and a pixel size of 0.″04. Figure 1 reveals a source with greater than 4.0σ significance with a peak flux of $9.9 \pm 2.3 \times 10^{-5}$ Jy/beam (uncorrected for magnification). The uncertainty and significance level was computed from the rms measured across a representative ≈2 × 2 arcmin field. The signal is seen within two independent frequency ranges (center panels in Figure 1) and the significance level is comparable to that claimed for Watson et al's $z \sim 7.5$ lensed system, although its observed flux is six times fainter. Taking into account the different magnification factors (see later), the intrinsic (lensing-corrected) peak fluxes are similar at $\approx 5 \times 10^{-5}$ Jy. Dividing the exposure into two independent halves, the significances of 3.2 and 3.4 are consistent with that of the total exposure.

To identify the likely source, we examined the final version of the reduced *HST* data of Abell 2744 (ACS and WFC3) acquired between 2013 November and 2014 July as part of the Frontier Fields program (ID: 13495, PI: Lotz), combining this with archival data from previous campaigns (ID: 11689, PI: Dupke; ID: 13386, PI: Rodney). Although there is some structure in the ALMA detection, it lies close to the source A2744_YD4 (F160W = 26.3) at R.A. = 00:14:24.9, decl. = −30:22:56.1(2000) first identified by Zheng et al. (2014). Correcting for an astrometric offset between *HST* positions and astrometry measured by the *Gaia* telescope (Gaia Collaboration et al. 2016), we deduce a small physical offset of ≃0.2 arcsec between the ALMA detection and the *HST* image.

2.2. Other Imaging Data

Deep K_s data are also available from a 29.3 hr HAWK-I image taken between 2013 October and December (092.A-0472, PI: Brammer), which reaches a 5σ depth of 26.0. *Spitzer* IRAC data obtained in channels 1 ($\lambda_c \sim 3.6\ \mu$m) and 2 ($\lambda_c \sim 4.5\ \mu$m) with 5σ depths of 25.5 and 25.0, respectively, carried out under DDT program (ID: 90257, PI: T. Soifer). We extracted the *HST* photometry on PSF-matched data using *SExtractor* (Bertin & Arnouts 1996) v2.19.5 in double image mode using the F160W map for the primary detection (Figure 1). To derive the total flux, we applied an aperture correction based on the F160W MAG_AUTO measure (see, e.g., Bouwens et al. 2006). The noise level was determined using several 0.2 arcsec radius apertures distributed around the source. The total K_s magnitude of 26.45 ± 0.33 was obtained using a 0.6 arcsec diameter aperture applying the correction estimated in Brammer et al. (2016). The uncertainty was estimated following a similar procedure to that adopted for the *HST* data. The *Spitzer* data were reduced as described in Laporte et al. (2014) using corrected Basic Calibrated Data (cBCD) and the standard reduction software MOPEX to process, drizzle, and combine all data into a final mosaic. As shown in Figure 2, four other galaxies are close to A2744_YD4, but only the other source within the X-shooter slit is comparably bright to A2744_YD4. We used GALFIT (Peng & Ho 2002) to deblend the two sources and to measure their IRAC fluxes. We fitted both IRAC ch1 and ch2 images assuming fixed positions, those measured from the F160W image. Our photometry of A2744_YD4 is consistent with that published previously by the AstroDeep team (Zheng et al. 2014; Coe et al. 2015 and Merlin et al. 2016).

2.3. SED Fitting

We used several SED fitting codes to estimate the photometric redshift of A2744_YD4 and hence its implied association with the ALMA detection. In each case, we fit all the available photometric data (*HST*-ACS, *HST*-WFC3, VLT HAWK-I, *Spitzer*).

First, we used an updated version of *Hyperz* (Bolzonella et al. 2000) with a template library drawn from Bruzual & Charlot (2003), Chary & Elbaz (2001), Coleman et al. (1980), and Leitherer et al. (1999) including nebular emission lines as described by Schaerer & de Barros (2009). We permitted a range in redshift ($0 < z < 10$) and extinction ($0 < A_v < 3$) and found the best solution at $z_{\mathrm{phot}} = 8.42^{+0.09}_{-0.32}$ ($\chi^2 \sim 1$), with no acceptable solution at lower redshift. Restricting the redshift range to $0 < z < 3$ and increasing the extinction interval to ($0 < A_v < 10$), we found a low-redshift solution at $z_{\mathrm{phot}}^{\mathrm{low}-z} = 2.17^{+0.03}_{-0.08}$ but with a significantly worse $\chi^2 \sim 9$ (Figure 3).

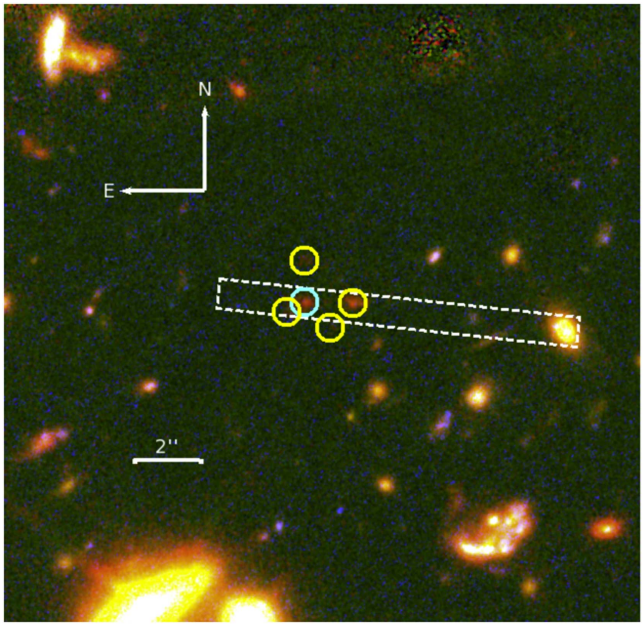

Figure 2. Position of the ALMA band 7 detected high-redshift galaxy A2744_YD4 (blue) with respect to other group members (yellow) suggested by Zheng et al. (2014). The X-shooter slit orientation is shown with the dashed white line. Although one other member of the group was targeted in the exposure, no confirming features were found in the data.

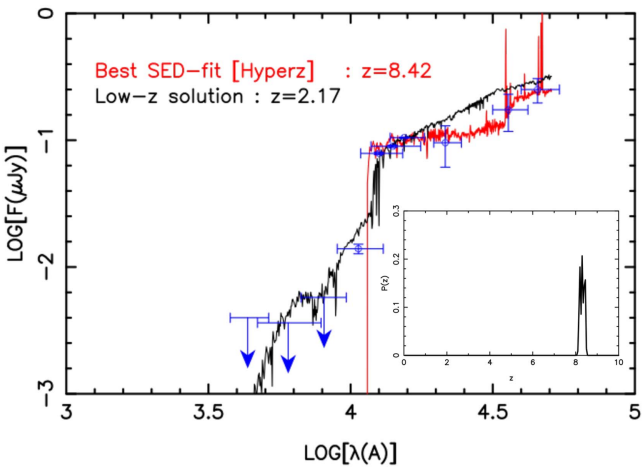

Figure 3. Spectral energy distribution of A2744_YD4. The red curve shows the best-fitting SED found by *Hyperz* with $z_{\rm phot} = 8.42^{+0.09}_{-0.32}$. The black curve shows a forced low-redshift solution derived when only a redshift interval from 0 to 3 is permitted. This has a likelihood >20 times lower. The inner panel displays the redshift probability distribution.

We also made use of the Easy and Accurate Zphot from Yale (EAZY; Brammer et al. 2008) software. The SED fits adopted the standard SED templates from EAZY, as well as those from the galaxy evolutionary synthesis models (GALEV; Kotulla et al. 2009) including nebular emission lines as described by Anders & Fritze-v. Alvensleben (2003). Adopting a large redshift range ($0 < z < 10$) with no prior assumptions on the extinction, the best fit has $z_{\rm phot} = 8.38^{+0.13}_{-0.11}$ in excellent agreement with that from *Hyperz*.

In summary, the photometry strongly supports a $z > 8$ solution. A low z solution is unlikely given the F814W-F125W > 3mag break as well as the low statistical likelihood.

3. Spectroscopic Follow-up

3.1. X-shooter Observations

Given the importance of confirming the presence of dust emission beyond $z \simeq 8$, we undertook a spectroscopic campaign using X-Shooter/VLT (ID: 298.A-5012, PI: Ellis). Between 2016 November 24 and 27, we secured 7.5 hr on-source integration with excellent seeing (≈0.6 arcsec). We used a 5 arcsec dither to improve the sky subtraction and aligned the slit so that a brighter nearby source could verify the blind offset (see Figure 2). The data were reduced using v2.8 of the ESO Reflex software combined with X-Shooter pipeline recipes v2.8.4.

We visually inspected all three arms of the X-Shooter (UVB, VIS, NIR) spectrum and identified one emission line at $\lambda = 11408.4$ Å with an integrated flux of $f = 1.82 \pm 0.46 \times 10^{-18}$ erg s^{-1} cm^{-2}. By measuring the rms at adjacent wavelengths, we measure the significance as $\approx 4.0\sigma$. We checked the reliability of the line by confirming its presence on two independent spectral subsets spanning half the total exposure time (Figure 4). These half-exposures show the line with significances of 2.7 and 3.0, consistent with that of the total exposure. No further emission lines of comparable significance were found. We explore two interpretations of this line at 11408 Å. It is either (1) one component of the [O II] doublet at a redshift $z \simeq 2.06$, or (2) Lyα at $z = 8.38$.

For (1), depending on which component of the [O II]λ3727, 3730 doublet is detected, we expect a second line at either 11416.9 Å or 11399.8 Å. No such emission is detected above the 1σ flux limit of 4.6×10^{-19} cgs. This would imply a flux ratio for the two components of ≈3.95 (2.02) at $1(2)\sigma$, greater than the range of 0.35–1.5 from theoretical studies (e.g., Pradhan et al. 2006).

For (2), although the line is somewhat narrow for Lyα (rest-frame width ≈20 km s^{-1}), its equivalent width deduced from the line flux and the F125W photometry is 10.7 ± 2.7 Å, consistent with the range seen in other $z > 7$ spectroscopically confirmed sources (Stark et al. 2017). We detect no flux above the noise level at the expected position of either the CIV and [O III] doublets at this redshift. However, at the expected position of the C III] doublet, we notice a very marginal ($\approx 2\sigma$) feature at $\lambda = 17914.7$ Å ($7.5 \pm 0.35 \times 10^{-19}$ erg s^{-1} cm^{-2}) seen on two individual sub-exposures. If this is C III]λ1907 Å (normally the brighter component) at $z_{\rm C\,III} = 8.396$, the Lyα offset of 338 ± 3 km s^{-1} would be similar to that for a $z = 7.73$ galaxy (Stark et al. 2017). The other component would be fainter than 5.0×10^{-19} erg s^{-1} cm^{-2}, consistent with theoretical studies of this doublet (e.g., Rubin et al. 2004).

Previous spectroscopy of A2774_YD4 was undertaken by the GLASS survey (Schmidt et al. 2016), who place a 1σ upper limit on any Lyα detection at 4.4×10^{-18} erg s^{-1} cm^{-2}, ≈2.4 times above our X-Shooter detection.

3.2. ALMA Observations

Only a few far-infrared emission lines lines are detectable for sources in the reionization era (see, e.g., Combes 2013). Only the [O III] 88 μm line at the $z = 8.38$ redshift of Lyα would be seen in the frequency range covered by our ALMA observations. Given the recent detection of this line in a $z \simeq 7.2$ Lyα emitter (Inoue et al. 2016), we examined our ALMA data for such a possibility. Searching our data in frequency space, we find a 4.0σ narrow emission line offset by 0.35 arcsec from the

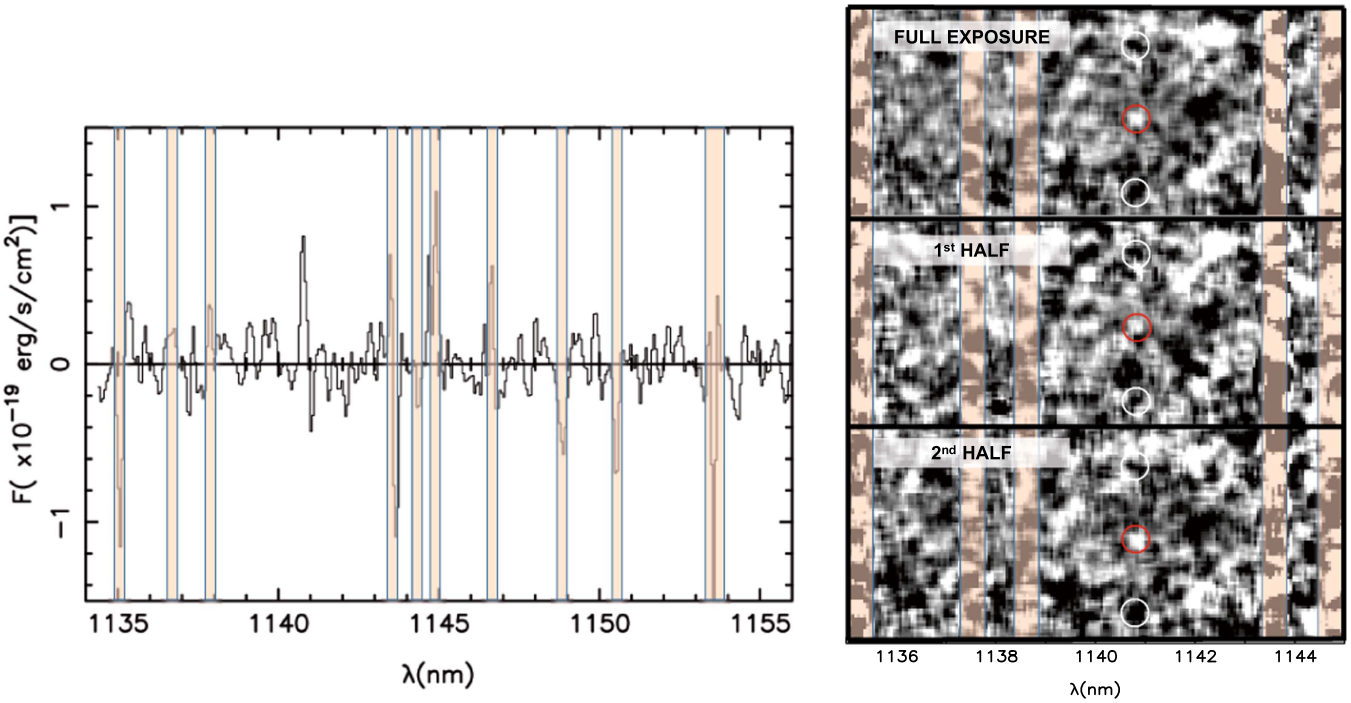

Figure 4. (left) Extracted 1D spectrum with OH night sky contamination indicated in orange. (right) 2D spectra separated into (top) the total exposure (7.5 hr on-source), (center) first half of the total exposure, (bottom) latter half of the total exposure.

astrometric position of A2744_YD4 at a frequency of 361.641 GHz. Dividing the exposure time in half, the line is detected with independent significances of 2.8 and 3.2, consistent with that of the total exposure. Assuming this line is [O III] 88 μm, the redshift would be $z = 8.382$ (see Figure 5), leading to a Lyα velocity shift of $\sim$70 km s^{-1} in good agreement with that observed in a $z \sim 7.2$ galaxy (Inoue et al. 2016). Fitting the emission line with a Gaussian profile, we derive a modest FWHM $= 49.8 \pm 4.2$ km s^{-1} implying an intrinsic width of $\simeq$43 km s^{-1}. The emission line luminosity is estimated at $1.40 \pm 0.35 \times 10^8 L_\odot$ without correction for magnification, which is $\approx$7 times fainter than that detected in Inoue et al.'s $z = 7.2$ source. The peak line flux of A2744_YD4 is consistent with that computed from simulations in Inoue et al. (2014, see their Figure 3). Compared to the aforementioned lower-mass source at $z = 7.2$, the narrower line width is perhaps surprising but may indicate its formation outside the body of the galaxy as inferred from the offset and recent simulations (Katz et al. 2016).

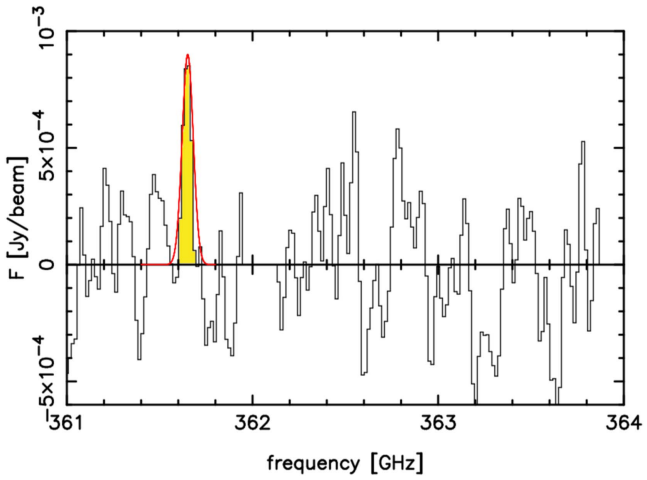

Figure 5. ALMA [O III]88 μm spectrum with a resolution of 25km s^{-1}. The best Gaussian profile is overplotted in red at the central frequency corresponding to a redshift of $z = 8.382$. The derived line width is $\approx$43 km s^{-1}.

4. Physical Properties

One of the main objectives of this study is to utilize the spectroscopic redshift as well as the ALMA band 7 detection to estimate accurate physical properties for A27744_YD4, and particularly to constrain the dust mass for an early star-forming galaxy.

4.1. Magnification

Estimating the magnification is critical to determine the intrinsic properties of any lensed source. Several teams have provided mass models for each of the six clusters. Moreover, a web tool[11] enables us to estimate the magnification for Abell2744_YD4 from parametric high-resolution models, i.e., version 3.1 of the CATS model (Richard et al. 2014), version 3 of Johnson et al. (2014), version 3 of Merten et al. (2011) and version 3 of GLAFIC (Ishigaki et al. 2015). We took the average value with error bars corresponding to the standard deviation: $\mu = 1.8 \pm 0.3$.

4.2. The Star Formation Rate (SFR) and Stellar and Dust Masses

The detection of dust emission in a $z = 8.38$ galaxy provides a unique opportunity to evaluate the production of dust, presumably from early supernovae in the first few 100 Myr since reionization began. The key measures are the dust and stellar masses and the likely average past SFR.

[11] https://archive.stsci.edu/prepds/frontier/lensmodels/#magcalc

We first estimate some physical properties based on the ALMA continuum detection using a simple modified blackbody SED with the dust temperatures ranging from 35 to 55 K and the dust emissivity fixed at $\beta \sim 2$. We found a total FIR luminosity ranging from 7.1 to 18.2 $\times$ 10^{10} $L_{\odot}$ and a dust mass ranging from 1.8 to 10.4 $\times$ 10^{6} $M_{\odot}$. These values are corrected for magnification and CMB heating.

We also ran an updated version of MAGPHYS (da Cunha et al. 2008) adapted for high-z galaxies (da Cunha et al. 2015). The code estimates the properties of A2744_YD4 in two steps. First, it generates a library of model SEDs at the redshift of our source ($z = 8.38$) in our 11 bands (7 from *HST*, the deep HAWK-I K_s band, the two first IRAC channels, and a synthetic filter of the ALMA band 7) for a wide range of variables including the SFR and dust content. We generated a total of about 9 million models, including ≈25,000 IR dust emission models. MAGPHYS then derives the likelihood distribution of each physical parameter by comparing the observed SED with all the models in the library. In this way, we derived the following properties: SFR $= 20.4^{+17.6}_{-9.5}$ $M_{\odot}$ yr^{-1}; a stellar mass $M_{\star} = (1.97^{+1.45}_{-0.66}) \times 10^{9}$ $M_{\odot}$; a dust mass $M_{\mathrm{dust}} = (5.5^{+19.6}_{-1.7}) \times 10^{6}$ $M_{\odot}$; and an extinction $A_v = 0.74^{+0.17}_{-0.48}$ with a dust temperature ranging from 37 to 63 K. The error bars refer to 1σ uncertainties. These values estimated with MAGPHYS using the full SED are consistent with those deduced solely from the ALMA continuum flux.

Although the uncertainties in these physical properties are large, our target is similar to the lensed source A1689-zD1 at $z \simeq 7.5$ studied by Watson et al. (2015). Watson et al. (2015) reports $M_{\star} = 1.7^{+0.7}_{-0.5} \times 10^{9}$ $M_{\odot}$ and SFRs 9^{+4}_{-2} $M_{\odot}$ yr^{-1}. Their specific star formation rates are thus similar ($1.04^{+10.2}_{-0.21} \times 10^{-8}$ yr^{-1} for A2744_YD4 and $0.6^{+1.1}_{-0.3} \times 10^{-8}$ yr^{-1} for A1689-zD1) implying a mean lifetime for a constant SFR of ≈100 Myr. However, A1689-zD1 has a significantly larger dust mass of $M_{\mathrm{dust}} = 4^{+4}_{-2} \times 10^{7}$ $M_{\odot}$. Possibly, this is a consequence of continuous star formation over a longer period together with more advanced chemical enrichment.

5. Discussion

Zheng et al. (2014) identified A2744_YD4 as one member of a group composed of five galaxies with similar colors and photometric redshifts. Although there is no spectroscopic information for the others members, conceivably this group is contained within a single ionized bubble, which may explain the detection of the Lyα emission in what is currently considered to be an epoch when the IGM is fairly neutral (Robertson et al. 2015). The putative group is contained within an area of 1.7 arcsec radius or 8.1 kpc (Figure 2). A second group member was included on the X-Shooter slit; although no emission was seen, it is over 1 mag fainter in continuum luminosity than A2744_YD4.

We finally turn to the implications of dust emission at such a high redshift. According to the most recent analyses of the history of cosmic reionization (Robertson et al. 2015; Mesinger et al. 2016; Planck Collaboration et al. 2016), significant star formation began at $z \simeq 10$–12, about 200 Myr before the epoch at which A2744_YD4 is being observed. The dust output and rate of early supernovae is of course highly uncertain but, for a past average SFR of 20 $M_{\odot}$ yr^{-1}, assuming a popular stellar initial mass function (e.g., Salpeter 1955) with a high-mass power-law slope of $\simeq -7/3$, we expect ≃0.2% of newly born stars to exceed 8 $M_{\odot}$ and produce Type II SNe. Assuming each SN produces around 0.5 $M_{\odot}$ of dust in its core (Matsuura et al. 2015), over 200 Myr this would yield around 4 $\times$ 10^{6} $M_{\odot}$ of dust in apparent agreement with the observations. However, this would not account for any dust lost to the system given typical velocities of ejection could be 10^{2-3} $\mathrm{km\,s}^{-1}$.

These speculations are as far as we can proceed given the current uncertainties. The most important conclusion is that ALMA clearly has the potential to detect dust emission within the heart of the reionization era and thus further measures of this kind, in conjunction with spectroscopic verification both using ALMA and soon the *James Webb Space Telescope*, offers the exciting prospect of tracing the early star formation and onset of chemical enrichment out to redshifts of 10 and beyond.

We acknowledge discussions with Dan Stark, Rob Ivison, Harley Katz, and Jason Spyromilio. N.L. and R.S.E. acknowledge support from the ERC Advanced Grant FP7/669253. D.Q. acknowledges support from a STFC Rutherford Grant (ST/M004139/2). F.E.B. acknowledges CONICYT-Chile (Basal-CATA PFB-06/2007, FONDECYT Regular 1141218), the Ministry of Economy, Development, and Tourism's Millennium Science Initiative through grant IC120009. I.P.F. acknowledges support from the grant ESP2015-65597-C4-4-R of the Spanish Ministerio de Economa y Competitividad (MINECO). This study is based on observations made at ESO's Paranal Observatory under programme ID 298.A-5012, on the following ALMA data: ADS/JAO.ALMA #[2015.1.00594], on observations obtained with the NASA/ESA *Hubble Space Telescope*, retrieved from the Mikulski Archive for Space Telescopes (MAST) at the Space Telescope Science Institute (STScI). ALMA is a partnership of ESO (representing its member states), NSF (USA) and NINS (Japan), together with NRC (Canada), NSC and ASIAA (Taiwan), and KASI (Republic of Korea), in cooperation with the Republic of Chile. The Joint ALMA Observatory is operated by ESO, AUI/NRAO and NAOJ. STScI is operated by the Association of Universities for Research in Astronomy, Inc. under NASA contract NAS 5-26555. We used gravitational lensing models produced by PIs Bradac, Natarajan & Kneib (CATS), Merten & Zitrin, Sharon, and Williams, and the GLAFIC and Diego groups. This lens modeling was partially funded by the *HST* Frontier Fields program conducted by STScI. STScI is operated by the Association of Universities for Research in Astronomy, Inc. under NASA contract NAS 5-26555.

References

Anders, P., & Fritze-v. Alvensleben, U. 2003, A&A, 401, 1063
Atek, H., Richard, J., Jauzac, M., et al. 2015, ApJ, 814, 69
Bertin, E., & Arnouts, S. 1996, A&AS, 117, 393
Bolzonella, M., Miralles, J.-M., & Pelló, R. 2000, A&A, 363, 476
Bouwens, R. J., Illingworth, G. D., Blakeslee, J. P., & Franx, M. 2006, ApJ, 653, 53
Bouwens, R. J., Illingworth, G. D., Oesch, P. A., et al. 2015, ApJ, 803, 34
Brammer, G. B., Marchesini, D., Labbé, I., et al. 2016, ApJS, 226, 6
Brammer, G. B., van Dokkum, P. G., & Coppi, P. 2008, ApJ, 686, 1503
Bruzual, G., & Charlot, S. 2003, MNRAS, 344, 1000
Chary, R., & Elbaz, D. 2001, ApJ, 556, 562
Coe, D., Bradley, L., & Zitrin, A. 2015, ApJ, 800, 84
Coleman, G. D., Wu, C.-C., & Weedman, D. W. 1980, ApJS, 43, 393
Combes, F. 2013, in ASP Conf. Ser. 476, New Trends in Radio Astronomy in the ALMA Era: The 30th Anniversary of Nobeyama Radio Observatory, ed. R. Kawabe, N. Kuno, & S. Yamamoto (San Francisco, CA: ASP), 23
da Cunha, E., Charlot, S., & Elbaz, D. 2008, MNRAS, 388, 1595
da Cunha, E., Walter, F., Smail, I. R., et al. 2015, ApJ, 806, 110
Ellis, R. S., McLure, R. J., Dunlop, J. S., et al. 2013, ApJL, 763, L7

Finkelstein, S. L., Ryan, R. E., Jr., Papovich, C., et al. 2015, ApJ, 810, 71
Gaia Collaboration, Brown, A. G. A., Vallenari, A., Prusti, T., et al. 2016, A&A, 595, A2
Inoue, A. K., Shimizu, I., Tamura, Y., et al. 2014, ApJL, 780, L18
Inoue, A. K., Tamura, Y., Matsuo, H., et al. 2016, Sci, 352, 1559
Ishigaki, M., Kawamata, R., Ouchi, M., et al. 2015, ApJ, 799, 12
Johnson, T. L., Sharon, K., Bayliss, M. B., et al. 2014, ApJ, 797, 48
Katz, H., Kimm, T., Sijacki, D., et al. 2016, MNRAS, submitted (arXiv:1612.01786)
Kotulla, R., Fritze, U., Weilbacher, P., & Anders, P. 2009, MNRAS, 396, 462
Laporte, N., Infante, L., Troncoso Iribarren, P., et al. 2016, ApJ, 820, 98
Laporte, N., Streblyanska, A., Clement, B., et al. 2014, A&A, 562, L8
Leitherer, C., Schaerer, D., Goldader, J. D., et al. 1999, ApJS, 123, 3
Lotz, J. M., Koekemoer, A., Coe, D., et al. 2016, arXiv:1605.06567
Matsuura, M., Dwek, E., Barlow, M. J., et al. 2015, ApJ, 800, 50
McMullin, J. P., Waters, B., Schiebel, D., Young, W., & Golap, K. 2007, in ASP Conf. Ser. 376, Astronomical Data Analysis Software and Systems XVI, ed. R. A. Shaw, F. Hill, & D. J. Bell (San Francisco, CA: ASP), 127
Merlin, E., Amorín, R., Castellano, M., et al. 2016, A&A, 590, A30
Merten, J., Coe, D., Dupke, R., et al. 2011, MNRAS, 417, 333
Mesinger, A., Greig, B., & Sobacchi, E. 2016, MNRAS, 459, 2342
Oke, J. B., & Gunn, J. E. 1983, ApJ, 266, 713
Peng, C. Y., Ho, L. C., Impey, C. D., & Rix, H.-W. 2002, AJ, 124, 266
Planck Collaboration, Ade, P. A. R., Aghanim, N., et al. 2016, A&A, 594 A13
Postman, M., Coe, D., Benítez, N., et al. 2012, ApJS, 199, 25
Pradhan, A. K., Montenegro, M., Nahar, S. N., & Eissner, W. 2006, MNRAS, 366, L6
Richard, J., Jauzac, M., Limousin, M., et al. 2014, MNRAS, 444, 268
Robertson, B. E., Ellis, R. S., Furlanetto, S. R., & Dunlop, J. S. 2015, ApJL, 802, L19
Rubin, R. H., Ferland, G. J., Chollet, E. E., & Horstmeyer, R. 2004, ApJ, 605, 784
Salpeter, E. E. 1955, ApJ, 121, 161
Schaerer, D., & de Barros, S. 2009, A&A, 502, 423
Schmidt, K. B., Treu, T., Bradač, M., et al. 2016, ApJ, 818, 38
Stark, D.-P. 2016, ARA&A, 54, 761
Stark, D. P., Ellis, R. S., Charlot, S., et al. 2017, MNRAS, 464, 469
Watson, D., Christensen, L., Knudsen, K. K., et al. 2015, Natur, 519, 327
Zheng, W., Shu, X., Moustakas, J., et al. 2014, ApJ, 795, 93